LBL-30294

Lawrence Berkeley Laboratory
UNIVERSITY OF CALIFORNIA

Presented at the XIV Annual Symposium on Nuclear Physics, Cuernavaca, Mexico, January 7–10, 1991, and to be published in the Proceedings

Sources and Characteristics of Complex Fragments in La-induced Reactions

P. Roussel-Chomaz, Y. Blumenfeld, R. Charity, M. Colonna, N. Colonna, B. Libby, K. Hanold, L. Moretto, G. Peaslee, and G. Wozniak

January 1991

U. C. Lawrence Berkeley Laboratory
Library, Berkeley

FOR REFERENCE

Not to be taken from this room

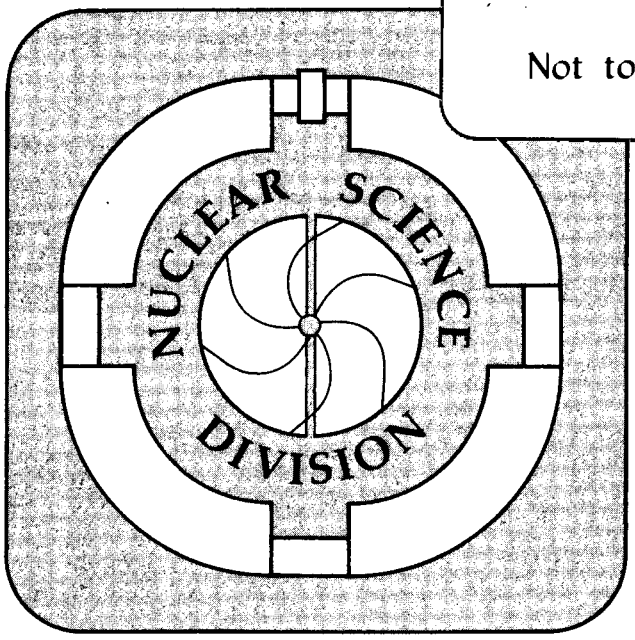

LBL-30294
Copy 1
Bldg. 50 Library.

Prepared for the U.S. Department of Energy under Contract Number DE-AC03-76SF00098

DISCLAIMER

This document was prepared as an account of work sponsored by the United States Government. While this document is believed to contain correct information, neither the United States Government nor any agency thereof, nor the Regents of the University of California, nor any of their employees, makes any warranty, express or implied, or assumes any legal responsibility for the accuracy, completeness, or usefulness of any information, apparatus, product, or process disclosed, or represents that its use would not infringe privately owned rights. Reference herein to any specific commercial product, process, or service by its trade name, trademark, manufacturer, or otherwise, does not necessarily constitute or imply its endorsement, recommendation, or favoring by the United States Government or any agency thereof, or the Regents of the University of California. The views and opinions of authors expressed herein do not necessarily state or reflect those of the United States Government or any agency thereof or the Regents of the University of California.

LBL - 30294

Sources and Characteristics of Complex Fragments in La-induced Reactions

P. Roussel-Chomaz, Y. Blumenfeld, R. Charity, M. Colonna, N. Colonna, B. Libby, K. Hanold, L. Moretto, G. Peaslee, and G. Wozniak

Nuclear Science Division
Lawrence Berkeley Laboratory
University of California
Berkeley, Ca 94720, USA

This work was supported by the Director, Office of Energy Research, Division of Nuclear Physics of the Office of High Energy and Nuclear Physics of the U.S. Department of Energy under Contract DE-AC03-76SF00098

Sources and Characteristics of Complex Fragments in La-induced Reactions

P. Roussel-Chomaz[a], Y. Blumenfeld[b], R. Charity[c], M. Colonna[d], N. Colonna, B. Libby[e], K. Hanold, L. Moretto, G. Peaslee[f], and G. Wozniak

Nuclear Science Division, Lawrence Berkeley Laboratory

1 Cyclotron Road, Berkeley, CA94720

Abstract

Complex fragment emission has been studied for a variety of reactions at intermediate energies. Multifragment events are shown to be associated with specific sources characterized by their mass and excitation energy through the incomplete fusion model. Excitation functions for the different multifragment decay channels are found to be almost independent of the system and the incident energy. Preliminary comparisons of the data with dynamical calculations followed by statistical decay calculations are discussed.

Introduction

When the subject is the production of complex fragments in heavy ion reactions, two main questions arise immediately: where do they come from and what is the mechanism involved in their formation?

At intermediate energies (E/A $\leq$ 50 MeV), two sources have been identified [1-4]: a fast, non-equilibrium source which produces light fragments at forward angles in normal kinematics and an equilibrium component, originating from the statistical decay of a compound nucleus via binary processes which cover the entire range of mass asymmetry in the exit channel. These compound nuclei are formed in complete or incomplete fusion reactions, depending on the incident energy and on the mass asymmetry of the system.

Within the incomplete fusion picture it is possible to correlate the mass and excitation energy of the product nucleus with the degree of fusion expressed by the source velocity. In reverse kinematics, for large impact parameters the nuclei formed are slightly heavier than the projectile and move at slightly lower velocity. As the impact parameter decreases, the projectile picks up more and more mass from the target, the velocity of the compound system decreases and its excitation energy increases. This correlation has been clearly observed for the 18 MeV/u La+Ni reaction [5], and it was possible with this method to study, at one incident energy, the decay properties of hot nuclei over a large excitation energy range. We shall try here to extend the method to ternary, quaternary, etc... events. We shall also compare our experimental results to some very preliminary results obtained by coupling a Landau-Vlasov type calculation [6] describing the dynamical stage of the collision with a statistical binary decay code [7] used to describe the deexcitation process.

[a] Permanent address: CEN Saclay, 91191 Gif sur Yvette Cedex France
[b] Permanent address: IPN Orsay, 91406 Orsay Cedex France
[c] Present address: Washington University, St Louis, MO 63130
[d] Present address: Universita di Catania, 95129 Catania, Italy
[e] Present address: University of Maryland, College Park, MD 20742
[f] Present address: NSCL, Michigan State University, E. Lansing, MI 48824

These results may help us to understand whether the decay mechanism is statistical or otherwise.

The experiment

We have studied complex fragment emission in the reactions induced by ^{139}La beams on different targets: ^{12}C,^{27}Al,^{40}Ca,^{51}V,^{nat}Cu, and ^{139}La. By using reverse kinematics, even the heaviest fragments have velocities large enough to be identified easily with simple ΔE-E telescopes. Furthermore the reaction products are focused in a narrow cone around the beam direction, therefore the detection efficiency is good even with a detection system of modest size.

Beams of 35, 40, 45 and 55 MeV/u ^{139}La were provided by the Lawrence Berkeley Laboratory BEVALAC. The intensity was 2-3x10^8 particles/pulse. (Some data obtained at GSI at 18 MeV/u and at MSU with ^{129}Xe beams will also be presented). The reaction products were detected in two arrays of 3x3 Si-Si-Plastic telescopes placed at 15° on each side of the beam axis, 37 cm far from the target. This detection system covered the angles between 3° and 28° in the horizontal plane and ±12.5° in the vertical plane. Each telescope had an active area of 4.5x4.5 cm^2 and its total area was 5.5x5.7 cm^2. Au foils (3mg/cm^2 thick) were placed in front of each telescope for electron suppression. Each telescope had three elements: a 300 μm thick position sensitive ΔE detector, a 5mm thick position sensitive Si-Li E detector and a 7.5 cm thick plastic scintillator with its photomultiplier tube.

In each telescope the two solid state detectors were positioned so that the 300 μm detector gave the position in the horizontal plane and the 5 mm detector gave the position in the vertical plane. The fragment positions were determined from resistive division across one face of the detector. Each device had 15 3mm-wide discrete strips and was therefore self-calibrated. For a point source, the angular resolution achieved was of the order of 0.5°.

To calibrate the Si detectors, several low intensity beams with the same A/Q ratios (namely $^{14}N^{4+}$, $^{28}Si^{8+}$, $^{56}Fe^{16+}$ and $^{84}Kr^{24+}$) were run at the same time directly into all the detectors, at several beam energies. We also utilized a low intensity ^{139}La beam to have a high-Z calibration point. The pulse height defect was taken into account, as well as the energy loss in the target and in the Au foils. The energy resolution obtained with such a procedure is around 1.5%. The charge resolution obtained from the ΔE-E measurement allowed identification of the Z value up to Z = 57. The mass corresponding to a given charge was estimated using the parametrization [8] $A=2.08*Z + 0.029*Z^2$.

Experimental results

To give an overview of the reaction mechanism, Fig. 1 presents for the 2-body events, the correlation between the velocities (normalized to the beam velocity) reconstructed for the source of the fragments by the relation $v_s=\Sigma m_i v_i/\Sigma m_i$ and the total charge detected, for six different energies ranging from 18 to 55 MeV/u and four entrance channel

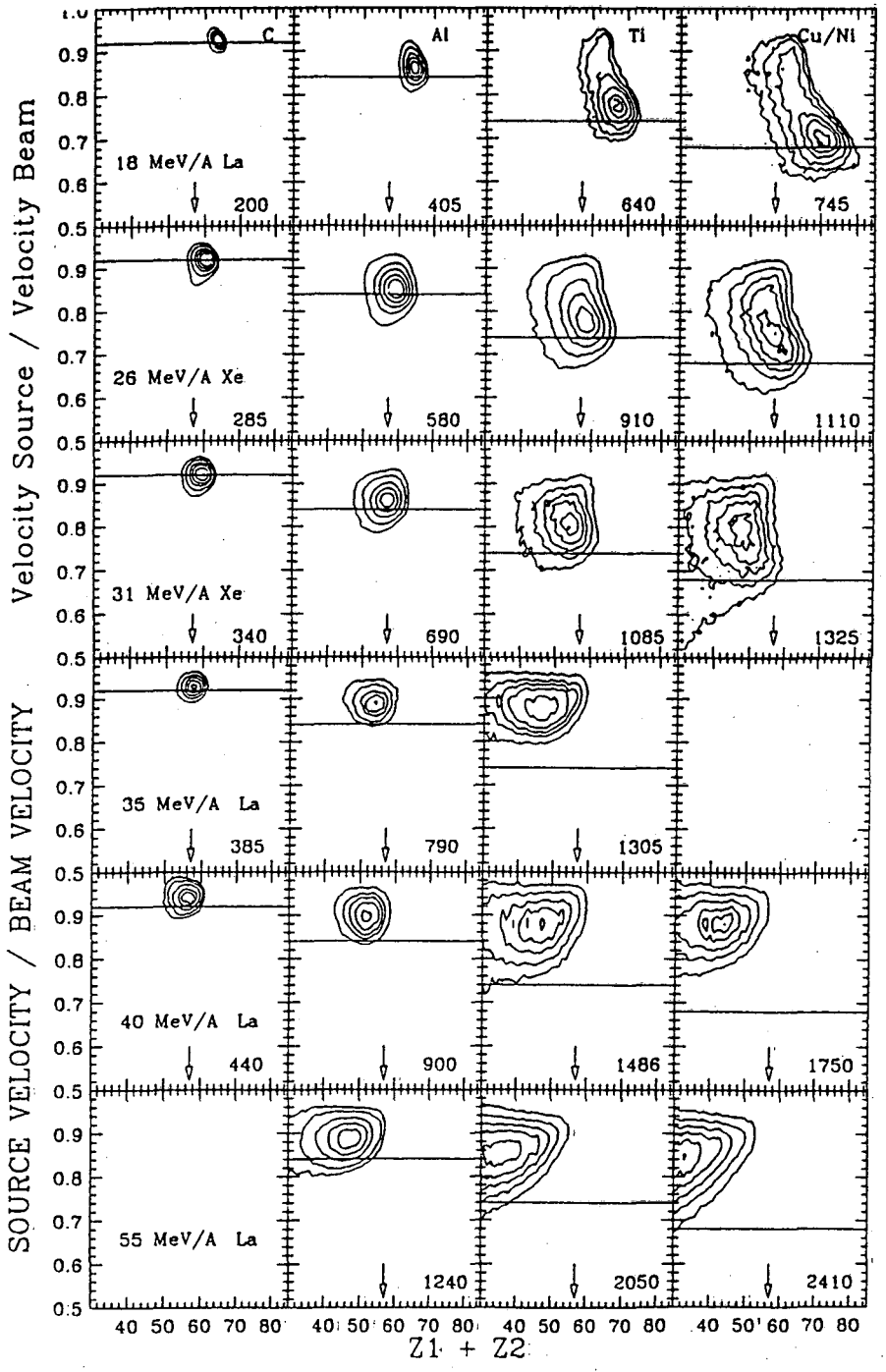

Fig. 1: Linear contour plots of the source velocity versus total detected charge for 2-fold coincidence events, for 6 incident energies and 4 different entrance channel asymmetries. The beam energy and the target are indicated in the first row and column; respectively. The total available energy in the c.m. system is indicated in the lower right of each frame. The horizontal lines indicate the complete fusion velocity for each system and the vertical arrows the projectile charge.

asymmetries. The data corresponding to Xe beams have been shifted by 3 Z-units to make the comparison easier ($\Delta Z_{La-Xe}=3$).

The first row corresponds to the most asymmetric system La/Xe + C, which has relatively low available energies in the center of mass system, and presents a very simple pattern. At 18 MeV/u, the source velocity distribution peaks at the value expected for complete fusion, which corresponds to the solid line, and the total charge detected is the total charge of the system. In this case, complete fusion has occurred and only neutrons have been evaporated. When the incident energy increases, the distributions move to higher source velocities and lower total detected charge. The higher velocity corresponds to the onset of incomplete fusion since in reverse kinematics, when the projectile picks up less mass from the target, the compound system is less slowed down and the measured source velocity is therefore higher. The same kind of description can be given for the Al target. The only difference is that due to the higher excitations energies that can be reached, the evaporation is more extensive and the detected charge is less than that of the primary compound nucleus, even at 18 MeV/u.

The pattern observed for the heavier targets is more complicated. At 18 MeV/u we observe a very nice illustration of the transition from complete fusion ($Z_1+Z_2 \approx Z_P+Z_T$) to incomplete fusion, with a ridge line going to lower secondary charge when the source velocity increases, which is again what is expected for incomplete fusion in reverse kinematics. As the incident energy increases, and the excitation energy available in the reaction increases, the pattern shifts towards lower Z values because of the evaporation process. At 35 MeV/u the pattern one obtains is upright, indicating that the system lost by evaporation as many nucleons as it had gained from the fusion with the target. The patterns observed for ^{51}V and ^{nat}Cu above 35 Mev/u are quite different, with a ridge line going to lower secondary detected charge when the source velocity decreases, which is the opposite to what was observed at lower incident energy.

To stay with binary events one can also look at the correlation between the measured charge for the two fragments. This kind of plot allows one to determine whether there are only two main fragments or more in the final state of the reaction. If the final state is really binary, the contour plots should be dominated by a band of events peaking at $Z_1+Z_2=Z_P+Z_T$. If the exit channel is actually multibody with one or several fragments not detected, the events should be distributed everywhere under the line.

The pattern observed on Fig.2 is very clear for La/Xe + C where the contour plots peak at values near the total charge of the system, thus illustrating the binary nature of the process. The band broadens and shifts towards smaller total charge as the incident energy increases, because of evaporation. In the case of Al this last effect becomes more important and at the highest incident energy a large fraction of the events are multibody with only two fragments detected. This is even more true for the heavier targets where the band at high Z_1+Z_2 disappears completely above 35 MeV/u.

We shall now consider n-fold events, i.e. events where n fragments are detected in coincidence, with n=2, 3, 4 and even 5 at 55 MeV/u.

Fig.3 presents the Z distributions for n-fold events for all the systems measured at 40 MeV/u. The plots obtained for 2-body events are nothing but the projection of Fig. 2 on the principal diagonal. For the ^{12}C target a narrow peak is observed, but as the mass of target increases,this peak broadens and shifts to lower detected charge. These effects arise

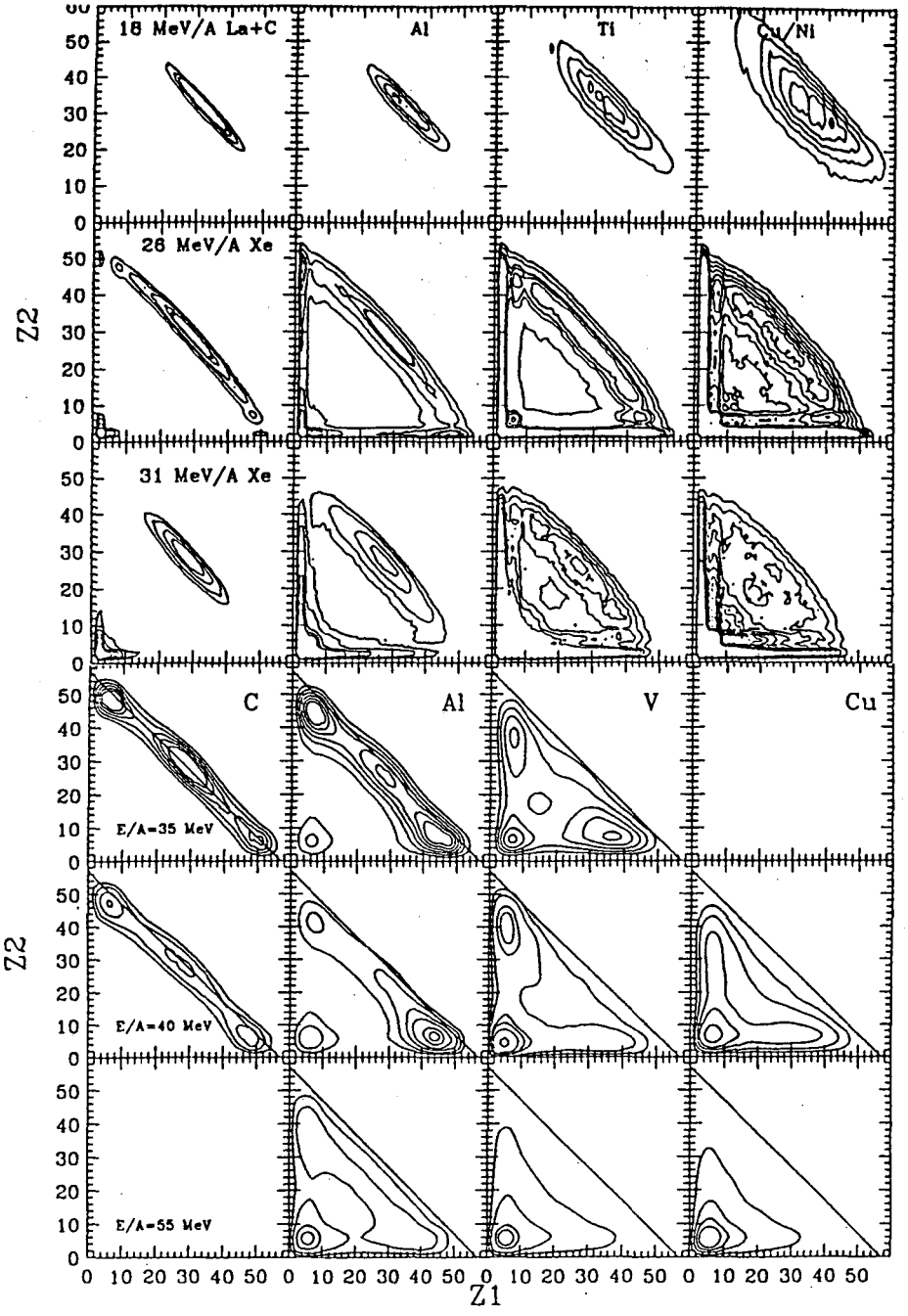

Fig. 2: Linear contour plots of Z_1 versus Z_2 for 2-fold coincidence events. On some of the plots the diagonal line indicate the charge of the projectile (Z_p=57).

from the larger range of mass transfers and from the increase of light particle evaporation due to the larger range of excitation energies available. The tail at low total detected charges also increases with the mass of the target, and this is related to the increase of higher n-fold events where only 2 fragments are detected. The same Z_{total} distribution plotted for 3-fold and 4-fold events presents a peak centered at approximatively the same value, but with a reduced tail to low Z_{total}, indicating that most of these events are complete.

In the following we will restrict ourselves to events where the total measured charge is higher than 30, in order to exclude those events where one fragment is clearly missing and to avoid biaising our kinematical reconstructions. Fig. 4 presents the source velocity distributions obtained at 40 MeV/u for all the targets and for the different fragment multiplicities. The observed peak broadens significantly when the mass of the target increases. This width has two different origins: incomplete fusion processes and the broadening from evaporation. This contribution has been estimated with the statistical code Gemini[9]. In the case of the ^{12}C target, the width can be explained almost entirely by light particle evaporation, but in the case of the heavier targets, a wide range of excitation energies contributes effectively to complex fragment emission. For a given target, the requirement of larger multiplicity of complex fragments selects out events with lower source velocities and therefore higher excitation energies. The same trend has been observed with Ne+Au at 60 MeV/u [10].

To study the behavior of hot nuclear systems as their excitation energy increases, excitation functions for the binary, ternary, etc. decay channels have been constructed. More precisely, Fig. 5 presents the evolution of the proportion of n-fold events with respect to the total number of coincidence events as a function of the excitation energy inferred from the source velocity through the incomplete fusion model, for four incident

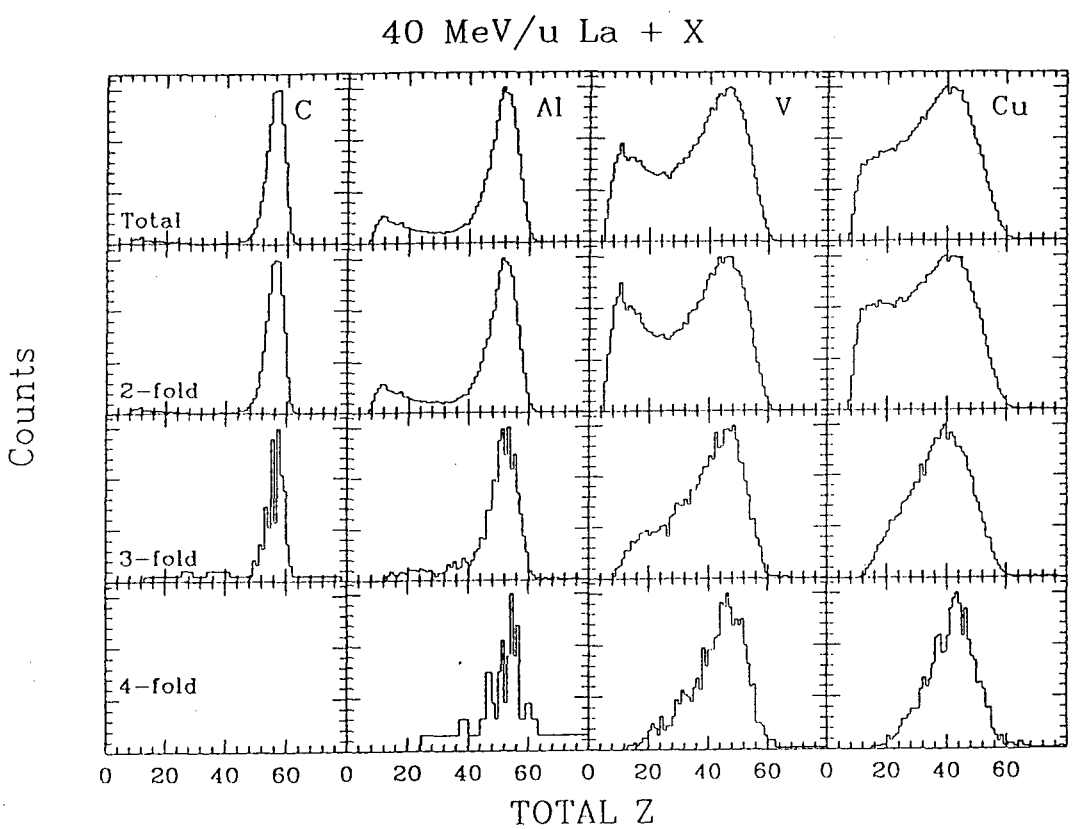

Fig. 3: Total detected charge for some of the systems measured at 40 MeV/u as a function of the multiplicity in the exit channel.

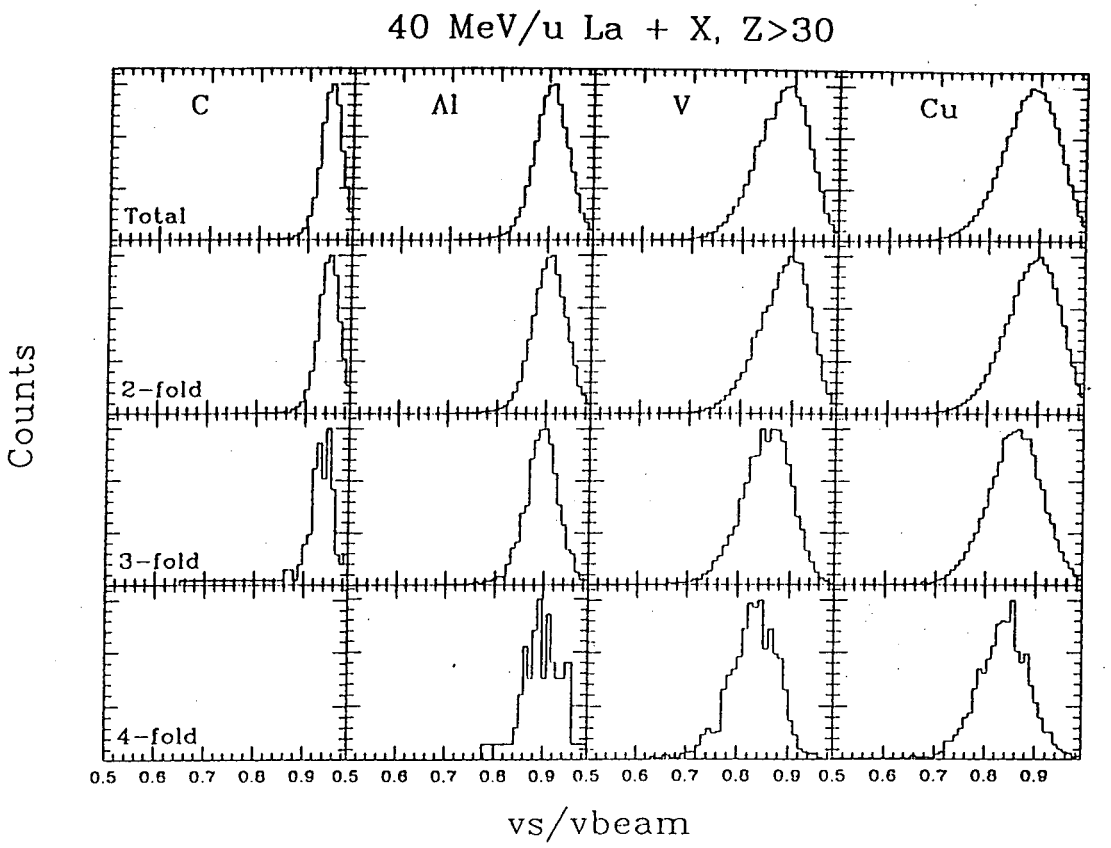

Fig. 4: Same as Fig. 3 for the source velocities expressed as the ratio of the source to the beam velocity.

energies. The picture obtained is quite striking. First, at all energies the 3-fold and 4-fold event probabilities (and 5-fold at 55 MeV/u) increase significantly up to excitation energies as high as 8 MeV/u. This energy dependence is a good indication that the relation between E^* and the source velocity is valid and also confirms that the width of the source velocity distribution is only partly due to light particle evaporation (if it were only particle evaporation, the excitation functions would be flat). Second, the increase observed in these excitation functions is smooth. We see no evidence for a phase transition towards nuclear cracking[11,12], and the data suggest that the decay of the hot nuclei under study is governed by the same mechanism up to an excitation energy approaching the total binding energy of these nuclei.

A closer look at Fig.5 shows some minor discrepancies, for the lightest targets, for which the points are low. In the case of ^{12}C this can probably be explained by the light particle evaporation which is a major contribution to the width of the source velocity distribution. This can also explain why in the case of ^{27}Al, the multi-fold probabilities at the highest excitation energies, which correspond to the tail of the source velocity distribution, fall slightly below those for the heavier targets. We have checked for the 35 MeV/u La + Ca data that these excitation functions were not skewed by our detection efficiency [9]. However, it has to be pointed out that due to preequilibrium processes not taken into account here, the excitation energy scale may be wrong by up to 30%, but these effects should only compress smoothly the energy scale.

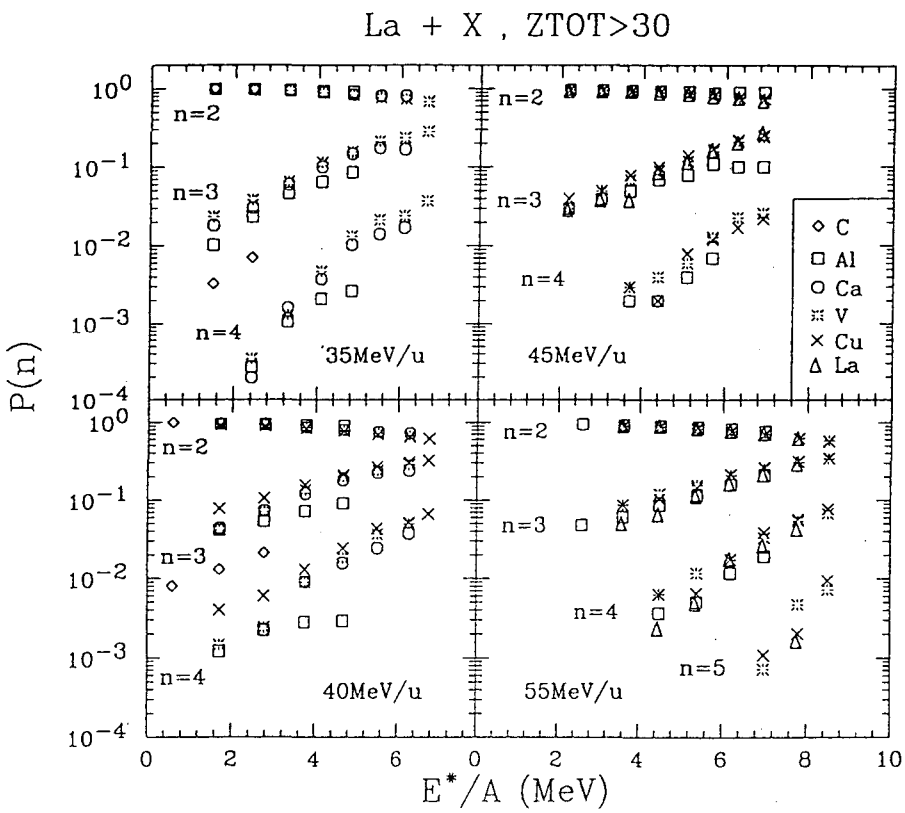

Fig. 5: Proportion of 2-3-4-5 fold events as a function of the excitation energy per nucleon for the systems studied at 4 different energies.

To conclude on these excitation functions, their independence with respect to target-projectile combination and to incident energy suggests a competition between the different decay channels independent of the entrance channel and therefore supports the idea of an intermediate system whose decay properties are mainly determined by its excitation energy and angular momentum.

Boltzmann-Nordheim-Vlasov calculations

It seems interesting to compare our experimental data with the predictions obtained for complex fragment emission with a self-consistent transport equation approach (Boltzmann-Nordheim-Vlasov or Landau-Vlasov). The two fundamental ingredients that enter the BNV equation are the self consistent mean field and the in-medium nucleon-nucleon cross section σ_{NN}. In the code we used [6], the mean field is given by the Coulomb interaction between protons plus a nuclear density dependent part of Skyrme type with parameters chosen to get a nuclear compressibility value K=200 MeV. The cross section σ_{NN} is assumed to be the free nucleon-nucleon cross section with an energy dependence parametrized from experimental data. An example of the evolution of the collision between La and Al at 55 MeV/u is presented on Fig. 6 as a function of time for different impact parameters .

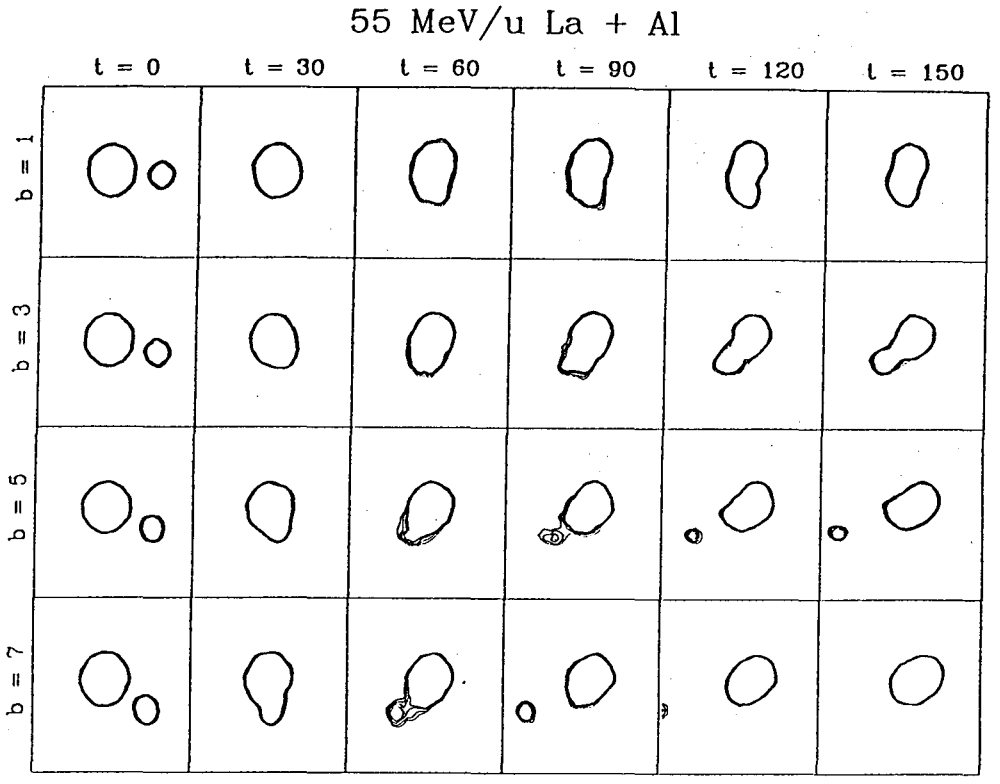

Fig. 6: La+Al collisions at 55MeV/u calculated with the BNV equation for several impact parameters (expressed in fm). The initial velocity axis (z) is horizontal and the impact parameter axis (x) is vertical. The times are expressed in fm/c. The lines represent equal density level in the (x,z) plane.

For the most central collisions, "complete fusion" occurs, accompanied by preequilibrium emission. At the end of the collisions only one heavy residue exists which is very elongated and will probably undergo fission (b = 3fm). For intermediate impact parameters, incomplete fusion occurs, where the target breaks into two pieces and part of the target is absorbed by the projectile. For larger impact parameters, the two incident nuclei merge together, but two centers can always be distinguished and, after a time depending on the impact parameter, the system separates into two fragments close in mass to the target and the projectile. Although this process is again accompanied by preequilibrium emission, its features are reminiscent of deep inelastic collisions as they are observed at low incident energies. For the heavier systems $^{139}La+^{51}V$ and $^{139}La+^{nat}Cu$ at 55 MeV/u, these calculations show the presence of a participant zone in addition to the projectile-like and target-like remnants for impact parameters between 5 and 7 fm, and therefore indicate the occurrence of participant-spectator type reactions.

Our purpose is now to compare our data where the fragments are detected "cold" with the fragments produced in the reactions predicted by this code. To achieve this, we stop the BNV calculations as soon as the compound system, if it exists, is equilibrated, or as soon as the 2 or 3 fragments produced in the exit channel are separated. Their

characteristics (A, Z, E^*, J, velocity, angle) are introduced as input in the statistical decay code Gemini[7].

The charge distribution obtained with this method for the system $^{139}La + ^{27}Al$ at 55 MeV/u is compared with the experimental cross sections in Fig. 7. The agreement is excellent in the region between Z = 18 and 45 but the calculation underpredicts the data in the intermediate mass region.

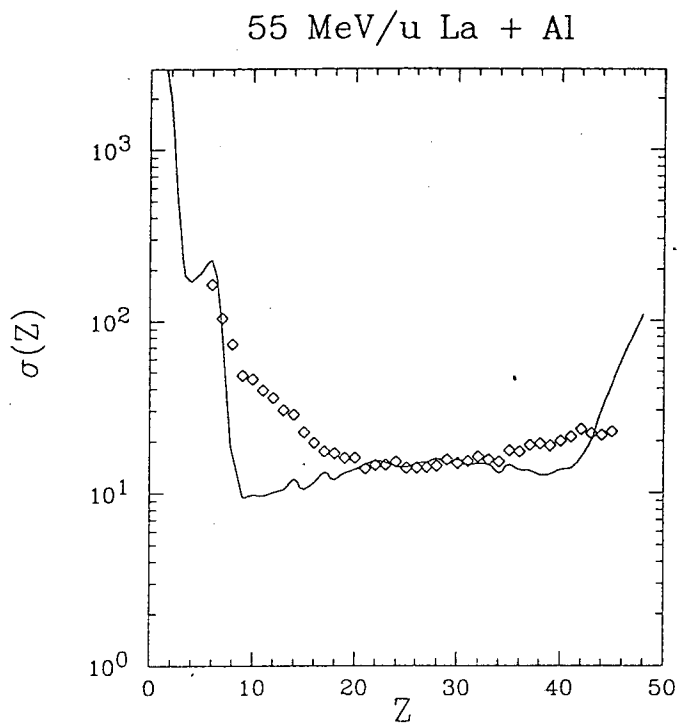

Fig. 7: Comparison of experimental integrated cross sections for La+Al at 55 MeV/u (diamonds) with the results of BNV + Gemini calculations (solid line , see text)

To summarize our preliminary results concerning the BNV calculations, they predict for asymmetric systems at intermediate energies the persistence of the mechanisms known below 10 MeV/u, accompanied by preequilibrium emission: complete or incomplete fusion for the most central impact parameters, and deep-inelastic processes for peripheral impact parameters. The same kind of conclusions have been drawn for the Ar+Ag reaction at 27 MeV/u [13]. For more symmetric systems we observe the onset of the fireball regime for intermediate and large impact parameters around 40 MeV/u.

Acknowledgements

This work was supported by the Director, Office of Energy Research, Division of Nuclear Physics of the Office of High Energy and Nuclear Physics of the US Department of Energy under contract DE-AC03-76SF00098. Apart from the authors, the following people participated in at least one of the experiments mentioned in this paper: D.Delis, K. Jing, M.Justice, M.A.McMahan, J.Meng, Q.Sui, G.D'Erasmo, E.Fiore, L.Fiore, G.Guarino, A.Pantaleo, V.Paticcio, S.Angius, I.Iori, A.Moroni, G.Santoruvo, W. Kehoe, A.Marchetti, A.Mignerey, D.G.Sarantites, L.G.Sobotka, A.Gobbi, K.D.Hidenbrand, M.Mohar, D.J.Morrissey.

References

[1] R.J. Charity et al., *Nucl. Phys.* A511, 59 (1990)
[2] M. Fatyga et al., *Phys. Rev. Lett.* 58, 2527 (1987)
[3] B.Borderie et al., *Phys. Lett.* B205, 26 (1988)
[4] E. Plagnol et al., *Phys.Lett.* B221, 11 (1989)
[5] N. Colonna et al., *Phys. Rev. Lett.* 62 , 1833 (1989)
[6] A. Bonasera et al., *Phys. Lett.* B244 , 169 (1990)
[7] R.J. Charity et al., *Nucl. Phys.* A483, 371 (1988)
[8] R.J. Charity et al., *Nucl. Phys.* A476, 516 (1988)
[9] Y. Blumenfeld et al., to be published in *Phys. Rev. Lett.*
[10] R. Bougault et al., *Phys. Lett.* B232 , 291 (1989)
[11] B. Borderie et al., to be published in *Ann. Phys.*

LAWRENCE BERKELEY LABORATORY
UNIVERSITY OF CALIFORNIA
INFORMATION RESOURCES DEPARTMENT
BERKELEY, CALIFORNIA 94720